



## Three-dimensional structure determination of a uniformly labeled molecule by frequency-selective dipolar recoupling under magic-angle spinning

Kaoru Nomura<sup>a,\*</sup>, K. Takegoshi<sup>a</sup>, Takehiko Terao<sup>a,\*\*</sup>, Kenichi Uchida<sup>b</sup> & Masatsune Kainosho<sup>c</sup>  
<sup>a</sup>Department of Chemistry, Graduate School of Science, Kyoto University, Kyoto 606-8502, Japan; <sup>b</sup>Department of Biosciences, School of Science and Engineering, Teikyo University, Utsunomiya 320-8551, Japan; <sup>c</sup>Department of Chemistry, Graduate School of Science, Tokyo Metropolitan University, Hachioji, Tokyo 192-0397, Japan

Received 23 December 1999; Accepted 6 April 2000

**Key words:** MAS, R2TR, selective dipolar recoupling, solid state NMR, three-dimensional structure determination, uniformly labeled powder sample

### Abstract

The complete three-dimensional (3D) structure of a glycyloleucine (Gly-Ile) molecule was determined by individually measuring six dihedral angles with a frequency-selective homonuclear dipolar recoupling method, R2TR (rotational resonance in the tilted rotating frame), using a powder sample of diluted uniformly <sup>13</sup>C, <sup>15</sup>N-labeled Gly-Ile. Each dihedral angle was obtained by recoupling a dipolar interaction between three or four bonds distant spins concerned or observing a dipolar correlation 2D powder pattern. The 3D structure of a Gly-Ile molecule was also determined by X-ray crystallography, and a good agreement with the NMR result was obtained. The results demonstrate that the R2TR method in a uniformly labeled powder sample can provide the 3D structure without the need to prepare a lot of selectively labeled samples.

### Introduction

Solid state NMR may provide important structural information without requiring long-range order nor solubility. In particular, measurements of dipolar interactions provide direct information on structures. With the aim of applying mainly to biological molecules, a lot of methods for dipolar recoupling under magic angle spinning (MAS) have been developed. While the non-selective measurements of dipolar couplings by broadband recoupling methods do not currently provide any quantitative structural information, selective measurements are practical and useful for obtaining local geometrical structures. In the latter, usually only one specific internuclear distance or dihedral angle is determined using a selectively isotope-labeled

powder sample. A large number of techniques for doubly labeled samples have been developed (Raleigh et al., 1988; Gullion and Schaefer, 1989; Tycko and Dabbagh, 1990; Bennett et al., 1992; Gullion and Vega, 1992; Fujiwara et al., 1993; Ishii and Terao, 1995; Lee et al., 1995; Sun et al., 1995; Takegoshi et al., 1996). However, if one tries to determine the three-dimensional (3D) structure composed of sizeable atoms by such approaches, many labeled samples must be prepared (Nishimura et al., 1998). On the other hand, if dipolar recoupling can be frequency-selectively realized, it allows us to recouple a specific dipolar interaction even in a uniformly labeled sample. Therefore, frequency-selective recoupling should have a potential for obtaining all the structural parameters necessary to determine the complete molecular structure one by one using a single sample, which significantly reduces experimental labor for preparing isotope-labeled samples.

\*Present address: Department of Chemistry, Graduate School of Science, Tokyo Metropolitan University, Hachioji, Tokyo 192-0397, Japan.

\*\*To whom correspondence should be addressed. E-mail: terao@kuchem.kyoto-u.ac.jp

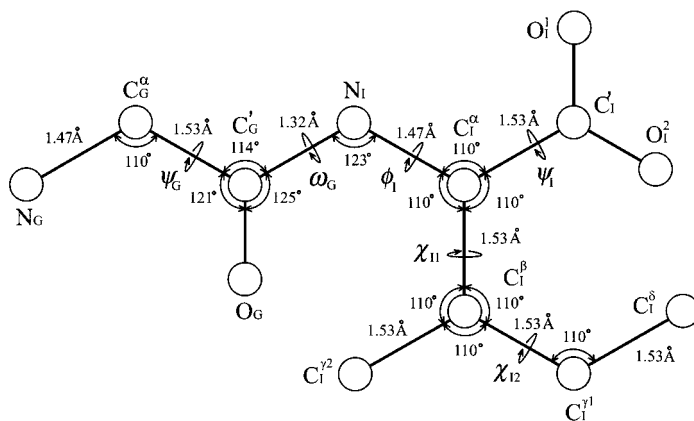


Figure 1. Schematic representation of a glycyloisoleucine molecule. Typical values of the bond distances (in Å) and the bond angles (in degrees) are shown, which were used to simulate experimental results and construct the three-dimensional structure of glycyloisoleucine. The glycine carbonyl and  $C_\alpha$  carbons are labeled as  $C'_G$  and  $C_G^\alpha$ , and the isoleucine carboxyl,  $C_\alpha$ ,  $C_\beta$ ,  $C_{\gamma 1}$ ,  $C_{\gamma 2}$ , and  $C_\delta$  carbons are as  $C'_I$ ,  $C_I^\alpha$ ,  $C_I^\beta$ ,  $C_I^{\gamma 1}$ ,  $C_I^{\gamma 2}$ , and  $C_I^\delta$ , respectively. The glycine amine and the isoleucine amide nitrogens are labeled as  $N_G$  and  $N_I$ , respectively, and the glycine carbonyl oxygen as  $O_G$ , and the two isoleucine carboxyl oxygens as  $O_I^1$  and  $O_I^2$ . The dihedral angles  $\phi_I$ ,  $\omega_G$ ,  $\psi_G$ ,  $\psi_I$ ,  $\chi_{11}$ , and  $\chi_{12}$  are also shown.

Rotational resonance ( $R^2$ ) (Andrew et al., 1963, 1966; Raleigh et al., 1987, 1988; Levitt et al., 1990) is a very simple and useful technique for selectively recoupling a particular homonuclear dipolar interaction which has been decoupled by MAS. Recoupling occurs when the spinning frequency  $\omega_R$  is adjusted to one  $n$ -th the resonance frequency difference. However,  $R^2$  is not a good means for selective recoupling in a uniformly labeled sample. When the chemical shift difference is small, the spinning speed must be slow. Not only does this yield many crowded spinning sidebands, but the other dipolar couplings cannot be sufficiently decoupled by such slow MAS. Furthermore,  $R^2$  is not frequency selective, but frequency-difference selective; therefore, if more than one carbon pair with the same separation exists, they are simultaneously recoupled. We extended  $R^2$  by applying an rf field with an intensity  $\omega_1$  and a frequency  $\omega_0$ , which we call R2TR (rotational resonance in the tilted rotating frame) (Takegoshi et al., 1995, 1997). Then, rotational resonance occurs in the tilted rotating frame under a zero-quantum (ZQ) condition ( $\omega_{eI} - \omega_{eS} = n\omega_R$ ), a single-quantum (SQ) condition ( $\omega_{eI} = n\omega_R$  or  $\omega_{eS} = n\omega_R$ ), or a double-quantum (DQ) condition ( $\omega_{eI} + \omega_{eS} = n\omega_R$ ), where  $\omega_{eX}$  is the effective field intensity for the  $X$  spin, with three experimentally adjustable parameters,  $\omega_1$ ,  $\omega_R$ , and  $\omega_0$  (Takegoshi et al., 1995). This diversity makes it possible, for example, to recouple a pair of spins with a small chemical shift difference while spinning fast enough to decouple all the other dipolar interactions. Furthermore, the R2TR

method can selectively recover a particular dipolar coupling by properly choosing the experimental parameters, even when more than two lines have equal chemical-shift differences.

In the present study, we have determined the complete structure of a glycyloisoleucine (Gly-Ile) molecule by R2TR using a powder sample of uniformly  $^{13}C, ^{15}N$ -labeled Gly-Ile molecules, including all the positions of carbons, nitrogens, and oxygens in both main chains and side chains. This is the first example of the complete structure determination of a molecule by solid state NMR; a preliminary report of this experiment has been presented (Nomura et al., 1999).

### Method of structure determination

We determine the 3D structure of a Gly-Ile molecule by obtaining the six dihedral angles shown in Figure 1. In this study,  $\psi_G$ ,  $\omega_G$ ,  $\phi_I$ ,  $\chi_{11}$ , and  $\chi_{12}$  are defined as dihedral angles  $N_G-C_G^\alpha-C'_G-N_I$ ,  $C_G^\alpha-C'_G-N_I-C_I^\alpha$ ,  $C'_G-N_I-C_I^\alpha-C_I^\beta$ ,  $C'_G-C_I^\alpha-C_I^\beta-C_I^{\gamma 1}$ , and  $C_I^\alpha-C_I^\beta-C_I^{\gamma 1}-C_I^\delta$ , respectively, by taking zero degrees for the *cis* conformation.  $\psi_I$  is defined as the angle between the  $N_I-C_I^\alpha$  bond and the  $O_I^1-C_I^\beta-O_I^2$  plane, being between  $0^\circ$  and  $180^\circ$ .

Except for  $\chi_{12}$ , each dihedral angle is determined by performing the R2TR dipolar recoupling experiment for a proper three- or four-bonds distant spin pair, assuming the typical bond lengths and angles shown in

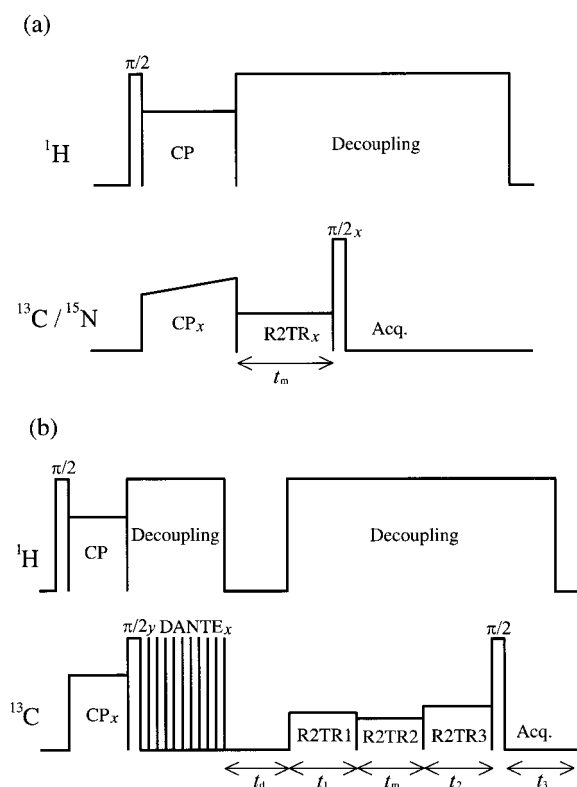


**Figure 2.** Pulse sequences to determine dihedral angles. (a) Dipolar recoupling experiment. After CP, an rf field satisfying a DQ condition for a particular pair of  $^{13}\text{C}$  spins is applied on-resonance to one of the spins for a recoupling time  $t_m$ . Then, the transverse magnetization of the spin is observed as a function of  $t_m$ . (b) 2D dipolar correlation experiment. After CP, the C magnetization in a four  $^{13}\text{C}$  spin (A-B-C-D) system is suppressed by a DANTE pulse train. The A-B and the C-D dipolar interactions are selectively recovered in the  $t_1$  and  $t_2$  periods, respectively. These dipolar powder patterns are correlated by transferring magnetization from A or B to C or D in the mixing period. The AB/CD dipolar correlation spectrum is obtained by observing the C magnetization in the detection period  $t_3$ .

Figure 1. We also assumed a planar configuration for the peptide plane.

Figure 2a shows the pulse sequence used in the dipolar recoupling experiments. During the recoupling period, the rf field satisfying a DQ condition is applied on-resonance to one of the pair spins concerned. Then, the recoupling-time ( $t_m$ ) dependence of the magnetization of the spin is observed, after a  $90^\circ$  pulse is applied to remove the possible small  $y$  component of the magnetization. The  $t_m$ -dependence of the magnetization is affected by  $T_{1\rho}$  relaxation; therefore, we corrected the data, measuring  $T_{1\rho}$  as described later.

To determine  $\chi_{12}$ , we made a 2D dipolar correlation experiment because of reasons mentioned later. In

the R2TR method, we can easily and quickly switch the dipolar interaction to be recoupled from one to another by changing  $\omega_1$  and  $\omega_0$  under a constant spinning speed. This makes it possible to realize a 2D experiment which correlates the AB and CD dipolar powder patterns in an A-B-C-D  $^{13}\text{C}$  spin system. The pulse sequence for this 2D experiment is shown in Figure 2b. After cross polarization (CP), the C magnetization is suppressed by a selective  $90^\circ$  (DANTE) pulse followed by a dephasing period ( $t_d$ ). In the first evolution period ( $t_1$ ) the AB dipolar interaction is selectively recoupled, in the mixing period the A or B magnetization is selectively transferred to the C or D spin, and in the second evolution period ( $t_2$ ) the C magnetization is evolved under the selectively recoupled CD dipolar interaction. The AB/CD dipolar correlated 2D powder pattern is selectively obtained by observing the C spin in the detection period ( $t_3$ ).

To recouple a specific dipolar interaction, we used a DQ R2TR condition with  $n=1$  ( $\omega_{eI} + \omega_{eS} = \omega_R$ ), except that a ZQ condition is used in the mixing period of the 2D dipolar correlation experiment for efficient polarization transfer. The other conditions of ZQ, SQ, and DQ ( $n > 1$ ) are not suitable for the present experiments for the following reasons. Firstly, to satisfy a ZQ condition, the chemical shift difference between a particular pair of spins must be larger than  $\omega_R$ . However, chemical shift differences of  $^{13}\text{C}$  or  $^{15}\text{N}$  spin pairs at a common range of magnetic field intensity are not so large as to satisfy a ZQ condition for  $\omega_R$  fast enough to completely decouple the other dipolar couplings. Secondly, under an SQ condition, both chemical shift anisotropies (CSAs) of the relevant carbons are dominantly recovered, obscuring the dipolar recoupling effect. Lastly, a DQ condition with  $n > 1$  requires a large rf-field intensity for  $\omega_R$  fast enough to decouple the other dipolar couplings, lowering the selectivity of recoupling.

Numerical simulations were done by a multistep method. Recoupling may take place even in off-R2TR conditions to some extent, and therefore we compensated for the incompleteness of selectivity by including a maximum of three spins into simulations in addition to the relevant two spins. We obtained empirical criteria of spins to be added in simulations by numerous calculations: Let us consider the selective recoupling of A and D in an A-B-C-D  $^{13}\text{C}$  system and assume the recoupling-time dependence of the D magnetization to be observed. In this case, not only all the four spins, but also all  $^{13}\text{C}$  spins directly bonded to D must be included. Further, a  $^{13}\text{C}$  spin within

about 2.5 Å from D should be included if the  $\omega_e$  difference between the spin and A is less than 1000 Hz. A  $^{13}\text{C}$  spin directly bonded to A should be included if the  $\omega_e$  difference between the spin and D is less than 1000 Hz.

Not only dipolar couplings but also CSA tensors contribute to the results. The  $^{13}\text{C}$  and  $^{15}\text{N}$  chemical shift parameters used for numerical simulations are collected in Table 1. The CSA tensors for the  $\text{sp}^2$  carbon are not very different from peptide to peptide. Hence, we used the mean values of  $\delta$  and  $\eta$  for the carbonyl carbons in AcGlyGlyNH<sub>2</sub>, AcGlyAlaNH<sub>2</sub>, AcGlyTyrNH<sub>2</sub>, and GlyGly·HCl (Oas et al., 1987a) for  $C'_G$ , and those for the carboxyl carbons in glycine (Haberkorn et al., 1981), L-alanine (Naito et al., 1981), L-serine (Naito et al., 1983), L-threonine (Janes et al., 1983), and L-asparagine (Naito et al., 1984) for  $C'_I$ . The values for  $N_G$  and  $N_I$  were determined from spinning sidebands observed at a low MAS speed. The directions of the principal axes of CSA tensors were assumed as follows: For  $C'_G$ , the  $\sigma_{33}$  axis is perpendicular to the  $\text{sp}^2$  plane (Veeman et al., 1984) and the  $\sigma_{22}$  axis makes an angle of 4.5° with the  $C'_G$ -O<sub>G</sub> bond toward the  $C'_G$ -C<sub>G</sub><sup>α</sup> bond (Oas et al., 1987a). For  $C'_I$ , the  $\sigma_{33}$  axis is perpendicular to the  $\text{sp}^2$  plane and the  $\sigma_{11}$  axis is along the C<sub>I</sub><sup>α</sup>-C<sub>I</sub>' bond (Veeman et al., 1984). For  $N_I$ , the  $\sigma_{22}$  axis is perpendicular to the peptide plane and the  $\sigma_{11}$  axis is along the C<sub>G</sub>'-N<sub>I</sub> bond (Oas et al., 1987b). For  $N_G$ , the  $\sigma_{33}$  direction is along the N<sub>G</sub>-C<sub>G</sub><sup>α</sup> bond direction and the  $\sigma_{11}$  axis is perpendicular to the N<sub>G</sub>-C<sub>G</sub><sup>α</sup>-C<sub>G</sub>' plane. For the aliphatic carbons, it will be shown that the CSA interactions do not significantly affect simulated results. Hence, we adopted likely values and directions for them.

## Experimental

The NMR experiments were performed on Chemagnetics CMX-300 and CMX-400 spectrometers operating at 75.6 MHz and 100.7 MHz, respectively, for  $^{13}\text{C}$  with Doty CPMAS probes having a 5  $\phi$  spinning system. The contact time for cross polarization was 2 ms and the recycling delay time between transients was 4 s. The rf-field strength for TPPM decoupling (Bennett et al., 1995) was 70~90 kHz and that for CP was 40~50 kHz. For the dipolar recoupling experiment, a precise adjustment of the rf-field intensity is required so as to accurately fulfill an appropriate R2TR condition for a selected spin pair. We calibrated the rf-field intensity by observing a nutation frequency under

MAS using adamantane. The rf-field inhomogeneity was estimated to be 2~3%, which barely affects the results; we used long caps supplied by Doty Scientific Inc. While the rf-field intensity for recoupling must be very stable in the present experiments, we found that the stability of an rf-field intensity in our spectrometers is insufficient in such low  $H_1$  as used in R2TR experiments. We have solved this problem for a weak pulse by controlling the intensity using a stable attenuator which we added and switching from the final power amplifier to a low power amplifier with high stability.

Uniformly  $^{13}\text{C}$ ,  $^{15}\text{N}$ -labeled Gly-Ile was prepared according to the following procedure. Boc-[ul- $^{13}\text{C}$ ,  $^{15}\text{N}$ ]Gly was prepared from [ul- $^{13}\text{C}$ ,  $^{15}\text{N}$ ]Gly (130 mg, 1.67 mmol) with di-*tert*-butylcarbonate (Moroder et al., 1976) (250 mg, 84%). [ul- $^{13}\text{C}$ ,  $^{15}\text{N}$ ]Ile-OMe·HCl was obtained from [ul- $^{13}\text{C}$ ,  $^{15}\text{N}$ ]Ile (230 mg, 1.67 mmol) with methanol and thionyl chloride (Brenner et al., 1953) (320 mg, quantitative). [ul- $^{13}\text{C}$ ,  $^{15}\text{N}$ ]Ile-OMe·HCl (320 mg, 1.67 mmol) was neutralized with an equimolar amount of *N*-methylmorpholine and then coupled with Boc-[ul- $^{13}\text{C}$ ,  $^{15}\text{N}$ ]Gly (250 mg, 1.40 mmol) by the DCC-HOBt method (Könich et al., 1970) (530 mg, quantitative). Boc-[ul- $^{13}\text{C}$ ,  $^{15}\text{N}$ ]Gly-[ul- $^{13}\text{C}$ ,  $^{15}\text{N}$ ]Ile-OMe was saponified with methanolic NaOH, followed by deprotection of the Boc group with 4 M HCl in ethyl acetate. The crude [ul- $^{13}\text{C}$ ,  $^{15}\text{N}$ ]Gly-[ul- $^{13}\text{C}$ ,  $^{15}\text{N}$ ]Ile was adsorbed on a Dowex 50-X8 column ( $\text{H}^+$  form) and eluted with 1.5 M NH<sub>4</sub>OH, and finally recrystallized from water (200 mg, 60%).

About 100 mg of a 10% uniformly  $^{13}\text{C}$ ,  $^{15}\text{N}$ -labeled sample, obtained by recrystallization of 100% uniformly  $^{13}\text{C}$ ,  $^{15}\text{N}$ -labeled Gly-Ile from deionized water with ninefold natural abundance material, was used for NMR measurements. For the 1D-dipolar recoupling experiment (Figure 2a), 16  $^{13}\text{C}$  FIDs or 64  $^{15}\text{N}$  FIDs were accumulated for each  $t_m$ . For the 2D correlation experiment (Figure 2b), the 32  $t_1$  data and the 15  $t_2$  data were collected after accumulating 16 FIDs for each ( $t_1$ ,  $t_2$ ). Total acquisition time was about 10 h.

An X-ray diffraction experiment was done as follows. A colorless prismatic crystal of Gly-Ile having approximate dimensions of 0.70 × 0.40 × 0.20 mm was used. All measurements were made on a Rigaku AFC7R diffractometer with filtered Cu-K<sub>α</sub> radiation. The final conventional *R* factor was 11.8%. We found that Gly-Ile crystallizes in the monoclinic space group *P*2<sub>1</sub>2<sub>1</sub>2<sub>1</sub>, *Z* = 4, with lattice constants of *a* = 6.432 Å, *b* = 30.018 Å, and *c* = 5.522 Å, and the

Table 1. Chemical shift parameters used for the numerical simulations of the R2TR dipolar recoupling experiments in glycyloisoleucine

	$C'_G$	$C'_I$	$C_G^\alpha$	$C_I^\alpha$	$C_I^\beta$	$C_I^{\gamma 1}$	$C_I^{\gamma 2}$	$C_I^\delta$	$N_I$	$N_G$
$\delta_{iso}^a$ (ppm)	178.9	169.3	64.0	40.3	36.3	26.7	17.0	12.4	120.9	23.1
$\delta^b$ (ppm)	-79.3 <sup>c</sup>	-71.0 <sup>d</sup>	20.0 <sup>e</sup>	-19.7 <sup>f</sup>	6.67 <sup>g</sup>	-12.3 <sup>h</sup>	-	-13.9 <sup>i</sup>	103.0 <sup>j</sup>	19.5 <sup>j</sup>
$\eta^b$	0.82 <sup>c</sup>	0.84 <sup>d</sup>	0.94 <sup>e</sup>	0.44 <sup>f</sup>	0.60 <sup>g</sup>	0.58 <sup>h</sup>	-	0.32 <sup>i</sup>	0.31 <sup>j</sup>	0.68 <sup>j</sup>

<sup>a</sup> $^{13}C$  and  $^{15}N$  isotropic chemical shifts were obtained with respect to  $Me_4Si$  and liquid  $NH_3$ , respectively.

<sup>b</sup>The anisotropy  $\delta$  and the asymmetry parameter  $\eta$  are defined as  $\delta = \delta_{zz} - \delta_{iso}$  and  $\eta = (\delta_{yy} - \delta_{xx})/\delta$ , where  $\delta_{iso}$  is the isotropic shift and  $|\delta_{yy} - \delta_{iso}| \leq |\delta_{xx} - \delta_{iso}| \leq |\delta_{zz} - \delta_{iso}|$ .

<sup>c</sup>Average of the values for the carbonyl carbons in some peptides (Oas et al., 1987a).

<sup>d</sup>Average of the values for the carboxyl carbons in glycine (Haberkorn et al., 1981), L-alanine (Naito et al., 1981), L-serine (Naito et al., 1983), L-threonine (Janes et al., 1983), L-asparagine (Naito et al., 1984).

<sup>e</sup>Values for the  $\alpha$  carbon in glycine (Haberkorn et al., 1981).

<sup>f</sup>Values for the  $\alpha$  carbon in L-alanine (Naito et al., 1981).

<sup>g</sup>Values for the  $\beta$  carbon in isobutane (Facelli et al., 1986).

<sup>h</sup>Values for the  $\alpha$ -methylene carbon in *n*-eicosane (VanderHart, 1976).

<sup>i</sup>Values for the methyl carbon in *n*-eicosane (VanderHart, 1976).

<sup>j</sup>Determined by the sideband analysis of a low-speed MAS spectrum.

four molecules in the unit cell are crystallographically equivalent.

## Results and discussion

### Signal assignment

Figure 3 shows a  $^{13}C$  CPMAS spectrum observed under a spinning speed of 17.5 kHz with TPPM decoupling together with a  $^{13}C$  COSY spectrum obtained with a CPMAS version of the conventional COSY sequence under TPPM decoupling. The observed eight signals ( $C_1$ - $C_8$ ) show the splitting due to the  $^{13}C$ - $^{13}C$  spin-spin couplings. As indicated in the figure, the  $C_2$  and  $C_4$  signals are connected with each other but isolated from the other carbons.  $C_2$  must obviously be assigned to the glycine carbonyl carbon ( $C'_G$ ) and  $C_4$  to the glycine  $C_\alpha$  carbon ( $C_G^\alpha$ ). The remaining signals  $C_1$ ,  $C_3$ ,  $C_5$ ,  $C_6$ ,  $C_7$ , and  $C_8$ , belonging to the isoleucine residue, can be assigned as  $C_1=C'_I$ ,  $C_3=C_I^\alpha$ ,  $C_5=C_I^\beta$ ,  $C_6=C_I^{\gamma 1}$ ,  $C_7=C_I^{\gamma 2}$ , and  $C_8=C_I^\delta$  from the connectivity and common knowledge of  $^{13}C$  chemical shifts. The observed isotropic chemical shifts are collected in Table 1.

A  $^{15}N$  CPMAS spectrum was recorded under a spinning speed of 17.5 kHz with TPPM decoupling (not shown). We assigned the resonance at 120.9 ppm to the amide nitrogen  $N_I$  and that at 23.03 ppm to the amine nitrogen  $N_G$ , referring to their typical isotropic shift values (Roberts et al., 1987).

### Dipolar recoupling experiments

In order to remove the influence of intermolecular dipolar couplings on the dipolar recoupling experiments, we used a sample of uniformly  $^{13}C$ ,  $^{15}N$ -labeled Gly-Ile 10-fold diluted with natural abundance material. The peaks from the natural abundance material were observed overlapping with those of the fully labeled molecules. To appreciate the contribution of the natural abundance material to the signal intensity observed in the dipolar recoupling experiment, we have done the dipolar recoupling experiment using natural abundance material. Since the dipolar recoupling between naturally abundant nuclei is negligibly small, this experiment corresponds to a  $T_{1\rho}$  measurement. As a result,  $T_{1\rho}$  was found to be much longer than the longest recoupling time used (10 ms), the magnetization of the natural abundance material being kept almost constant during  $t_m$ . Therefore, in the recoupling-time dependence experiments for the 10% uniformly labeled sample, we simply subtract 10% of the intensity at  $t_m = 0$  from the intensity observed at each recoupling time  $t_m$ .

Further, we must take account of the relaxation effect of the labeled material during the recoupling time  $t_m$ . To do so, we did the same experiment except for shifting the spinning frequency by  $\sim 500$  Hz from the R2TR condition. Subtracting the natural abundance contribution from the time dependence of the magnetization, we obtained  $T_{1\rho}$  for uniformly  $^{13}C$ ,  $^{15}N$ -labeled molecules. Then, the relaxation effect can be removed from the experimental data from which the natural abundance contribution has been subtracted, by mul-

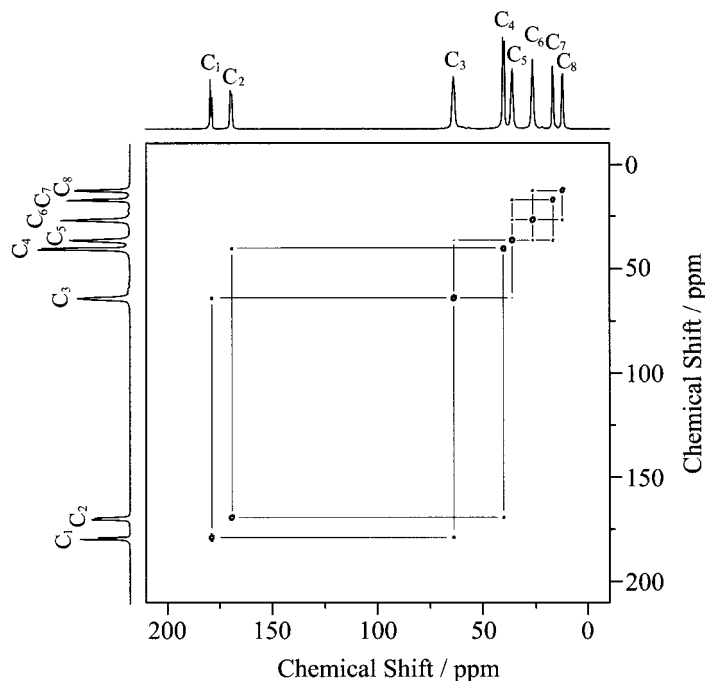


Figure 3.  $^{13}\text{C}$  COSY spectrum of uniformly  $^{13}\text{C}$ ,  $^{15}\text{N}$ -labeled glycyllsleucine. It was obtained under a spinning speed of 17.5 kHz and TPPM decoupling.

tipling the data by  $\exp(t_m/T_{1\rho})$ . In all the dipolar recoupling data shown below, both the subtraction of the natural abundance contribution and the correction for the relaxation effect have been done.

$\psi_G$  angle: The  $\psi_G$  angle was obtained through a dipolar recoupling experiment for  $\text{N}_G$  and  $\text{N}_I$ . The recoupling was achieved by applying an rf field satisfying a DQ condition under  $\omega_R = 17.5$  kHz: an rf field with intensity 8300 Hz was applied on-resonance to  $\text{N}_G$  during the recoupling period  $t_m$ . Figure 4a shows the recoupling-time dependence of the spin-locked magnetization of  $\text{N}_G$ . The root-mean-square deviation (rmsd) between the experimental data and the curves calculated for various  $\psi_G$  is shown in Figure 4b, and from the minimum,  $\psi_G$  was determined to be  $180^\circ$ . In the present approach, however, recoupling-time dependence is insensitive to the dihedral angle around  $0^\circ$  and  $180^\circ$ , displaying a very broad minimum. Nevertheless, the  $\Delta\chi^2$  plot shown in Figure 4b indicates that the 68% confidence interval ( $\Delta\chi^2 < 1$ ) is still  $\pm 10^\circ$ . The recoupling-time dependence calculated for  $\psi_G = 180^\circ$  is represented in Figure 4a.

Here, we examine to what extent the assumptions for the chemical shift tensors lead to error in the determination of  $\psi_G$ . We assumed that the direction

of the  $\sigma_{11}$  axis for the amide nitrogen is parallel to the peptide bond. While this is almost the case in general, in some cases, it deviates from the peptide bond direction to the  $\text{N}-\text{C}_\alpha$  direction by a maximum of about  $10^\circ$  (Oas et al., 1987a). We found that this amount of deviation in the  $\sigma_{11}$  direction of the  $\text{N}_I$  CSA tensor hardly changes the simulation curve, and that the deviation of  $10^\circ$  in the  $\sigma_{33}$  axis for  $\text{N}_G$  from the  $\text{C}_G^\alpha-\text{N}_G$  bond direction does not change it either. However, changing the CSA parameters ( $\delta, \eta$ ) = (103.0 ppm, 0.31) of  $\text{N}_I$  to those for the amide nitrogens in AcGlyTyrNH<sub>2</sub> (( $\delta, \eta$ ) = (96.4 ppm, 0.26)), or GlyGly-HCl (( $\delta, \eta$ ) = (101.0 ppm, 0.02)) (Oas et al., 1987b) results in the best-fit values of  $\psi_G = \pm 154^\circ$  or  $\pm 159^\circ$ , respectively, which are considerably different from the above value of  $180^\circ$ . As shown by this result, the recoupling-time dependence for  $\text{N}_I$  is sensitive to the CSA parameters  $\delta$  and  $\eta$ , particularly around  $\psi_G = 180^\circ$ , because the  $^{15}\text{N}-^{15}\text{N}$  dipolar interaction is the weakest for  $\psi_G = 180^\circ$  and, moreover, the recoupling-time dependence is insensitive to the dihedral angle around  $180^\circ$ . Therefore, it is desirable to measure the CSA parameters of  $\text{N}_I$  and use them in the simulations for determining  $\psi_G$  precisely. Note, however, that the averages of the CSA parameters of the amide nitrogens in AcGlyGlyNH<sub>2</sub>,

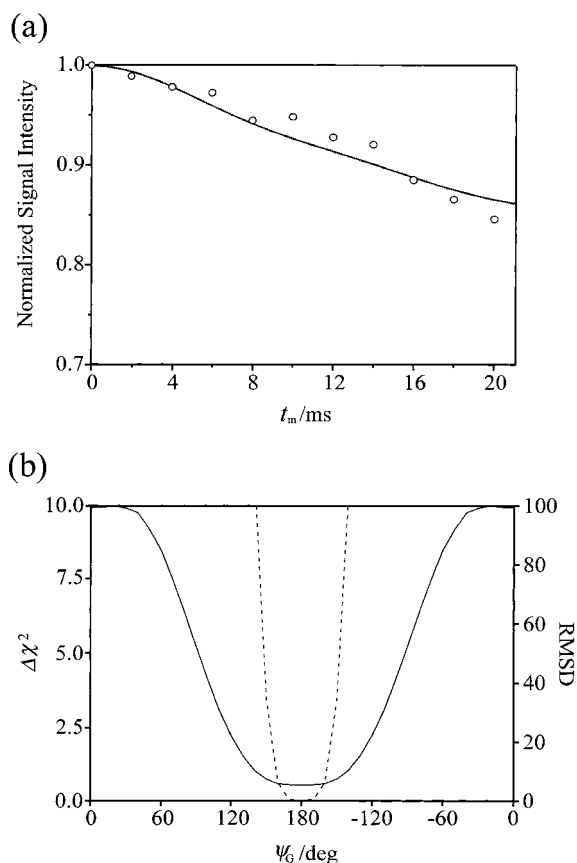


Figure 4. (a) Recoupling-time dependence of the normalized magnetization of  $N_G$  in 10% uniformly  $^{13}\text{C},^{15}\text{N}$ -labeled glycyloisoleucine. The dipolar recoupling experiment was carried out using the pulse sequence in Figure 2a under an R2TR condition ( $\omega_{eI} + \omega_{eS} = \omega_R$ ) satisfied for  $N_G$  and  $N_I$  by applying an rf field with intensity 8300 Hz on-resonance to the  $N_G$  carbon under MAS with  $\omega_R = 17.5$  kHz. Experimental points are shown by circles. The standard deviation for each point is ca.  $\pm 0.05$ . The curves are calculated for the dihedral angle  $\psi_G$  of  $180^\circ$ .  $T_{1\rho}$  was determined to be 70 ms by an off-R2TR experiment, and used to remove the relaxation effect from the dipolar recoupling data. (b) Dihedral angle ( $\psi_G$ ) dependence of rmsd (solid line) between the experimental (Figure 4a) and simulated data and of  $\Delta\chi^2$  (dashed line).

AcGlyAlaNH<sub>2</sub>, AcGlyTyrNH<sub>2</sub>, and GlyGly·HCl (Oas et al., 1987b) give  $(\delta, \eta) = (103.2 \text{ ppm}, 0.22)$ , which are similar to the observed values, and in fact, lead to the same  $\psi_G$  value of  $180^\circ$  as above.

$\omega_G, \phi_I,$  and  $\psi_I$  angles: Figure 5a shows the observed recoupling-time dependence of the magnetization of  $C'_I$  under a DQ condition satisfied between the resonances of  $C'_G$  and  $C'_I$ , where an rf field with intensity 8500 Hz was applied on-resonance to the  $C'_I$  carbon while spinning with  $\omega_R = 17.054$  kHz. Since

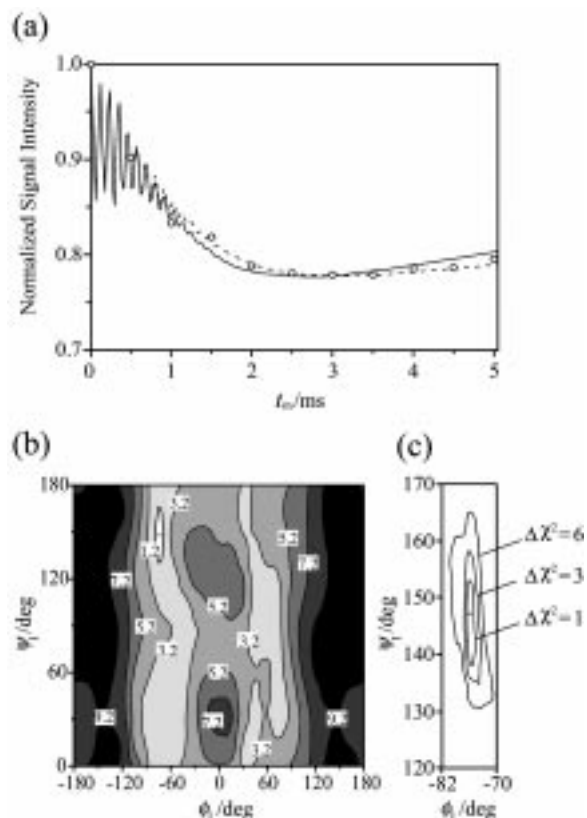


Figure 5. (a) Recoupling-time dependence of the normalized magnetization of  $C'_I$  in 10% uniformly  $^{13}\text{C},^{15}\text{N}$ -labeled glycyloisoleucine. The dipolar recoupling experiment was carried out using the pulse sequence in Figure 2a under an R2TR condition ( $\omega_{eI} + \omega_{eS} = \omega_R$ ) satisfied for  $C'_I$  and  $C'_G$  by applying an rf field with intensity 8500 Hz on-resonance to the  $C'_I$  carbon under MAS with  $\omega_R = 17.054$  kHz. Experimental points are shown by circles. The standard deviation for each point is ca.  $\pm 0.03$ . The solid line is the curve calculated for the dihedral angles  $(\omega_G, \phi_I, \psi_I) = (180^\circ, -76^\circ, 147^\circ)$ , whereas the dotted line for  $(\omega_G, \phi_I, \psi_I) = (0^\circ, -86^\circ, 167^\circ)$ .  $T_{1\rho}$  was determined to be 500 ms for  $C'_I$  in 10% uniformly  $^{13}\text{C},^{15}\text{N}$ -labeled glycyloisoleucine, and used to correct the experimental data. (b) The contour plot of rmsd between the experimental spectrum (Figure 5a) and the simulations for various sets of  $(\phi_I, \psi_I)$  and  $\omega_G = 180^\circ$ . The global minimum is indicated by a dot. (c) Dihedral angles  $(\phi_I$  and  $\psi_I)$  dependence of  $\Delta\chi^2$  for  $\omega_G = 180^\circ$ .

peptide planes take the *trans* configuration except for cyclic peptides or peptides with proline, we assume  $\omega_G$  to be  $180^\circ$ . If only the dipolar interaction between  $C'_G$  and  $C'_I$  contributes to the result, only the absolute value of the dihedral angle  $\phi_I$  can be determined from this experiment. In the present case, however, the large CSAs of both carbons and the relative orientations between the CSA tensors and the dipolar vector would significantly affect the experimental result. Hence, there may be a good chance of

determining not only  $\phi_I$  but also  $\psi_I$ . Therefore, we simulated the experimental curve, taking  $\phi_I$  and  $\psi_I$  as adjustable parameters. Furthermore, due to the imperfect selectivity of R2TR, three carbons,  $C'_G$ ,  $C'_I$ , and  $C'_I^\beta$ , do affect the recoupling-time dependence appreciably, so that they were included in addition to  $C'_G$  and  $C'_I$  in the calculation of the dipolar interactions. Figure 5b shows the contour plot of rmsd between the experimental data and the curves calculated for various  $\phi_I$  and  $\psi_I$ . From the global minimum,  $\phi_I$  and  $\psi_I$  were determined to be  $-76^\circ$  and  $147^\circ$ , respectively. It is worthy to point out here that if the recoupling-time curve depends only on  $C'_G$  and  $C'_I$ ,  $(\phi_I, \psi_I)$  and  $(-\phi_I, -\psi_I$  or  $180 - \psi_I)$  give identical results. However, the  $\Delta\chi^2$  values around  $(\phi_I, \psi_I) = (76^\circ, 33^\circ)$  are large (ca. 34). This apparent asymmetry comes from the inclusion of the outer carbons  $C'_G$ ,  $C'_I$ , and  $C'_I^\beta$ . Hence, we could uniquely determine both  $\phi_I$  and  $\psi_I$ . Figure 5c shows  $\Delta\chi^2$  around the global minimum; the 68% confidence regions ( $\Delta\chi^2 \sim 1$ ) for  $\phi_I$  and  $\psi_I$  are  $(-77^\circ \sim -75^\circ)$  and  $(138^\circ \sim 153^\circ)$ , respectively. The reason why  $\phi_I$  is precisely determined but  $\psi_I$  is not is because the dipolar coupling directly contributes to the determination of  $\phi_I$ , but  $\psi_I$  is obtained only through the relative orientation of the  $C'_I$  CSA tensor to the other tensors. The result of the recoupling experiment for  $C'_G$  and  $C'_I$  indicates that one dipolar recoupling experiment per amino acid residue is enough to determine dihedral angles ( $\psi, \phi$ ) which provide the 3D backbone structure of a peptide. In Figure 5(a) the recoupling-time dependence is shown calculated for the best-fit parameter set  $(\phi_I, \psi_I) = (-76^\circ, 147^\circ)$ . The rapid oscillation in the initial part of the simulated curve is caused by the presence of CSA and understood as the spinning sidebands in the tilted rotating frame, whose frequencies are given approximately by  $|\omega_1 - n\omega_R|$  ( $n$  is an integer) (Takegoshi et al., 1997). In experiments, however, we found that this oscillation is damped quickly within a few milliseconds due to rf-field inhomogeneity. Therefore, we damped this oscillation in the simulation to the same extent as the experimental data.

The large CSAs and the tensor orientations for the  $C'_G$  and  $C'_I$  carbons affect the recoupling behavior. Therefore, we examine the validity of the use of the CSA tensors assumed for  $C'_G$  and  $C'_I$  in the above simulations. First, as for  $C'_G$ , the  $\sigma_{22}$  axis direction was assumed to make an angle of  $4.5^\circ$  with the  $C'_G=O_G$  bond toward the  $C'_G-C'_G$  bond. Actually, it is along the  $C'=O$  bond direction in AcGlyGlyNH<sub>2</sub> and AcGlyAlaNH<sub>2</sub>

and deviates to the  $C'-C_\alpha$  bond direction about  $6^\circ$  and  $12^\circ$  in AcGlyTyrNH<sub>2</sub> and GlyGly·HCl, respectively (Oas et al., 1987a). The CSA parameters were assumed to be  $(\delta, \eta) = (-79.3 \text{ ppm}, 0.82)$ , while they are  $(-81.6 \text{ ppm}, 0.72)$ ,  $(-82.3 \text{ ppm}, 0.69)$ ,  $(74.7 \text{ ppm}, 0.94)$ , and  $(-80.9 \text{ ppm}, 0.82)$  for AcGlyGlyNH<sub>2</sub>, AcGlyAlaNH<sub>2</sub>, AcGlyTyrNH<sub>2</sub>, and GlyGly·HCl, respectively (Oas et al., 1987a). Simulating the experimental result using the individual CSA parameters and orientations, we obtained the best-fit values of  $(\phi_I, \psi_I) = (-76^\circ, 148^\circ)$ ,  $(-76^\circ, 148^\circ)$ ,  $(-71^\circ, 144^\circ)$ , and  $(-78^\circ, 139^\circ)$ , for AcGlyGlyNH<sub>2</sub>, AcGlyAlaNH<sub>2</sub>, AcGlyTyrNH<sub>2</sub>, and GlyGly·HCl, respectively. As for the tensor orientation of  $C'_I$ , we assumed the  $\sigma_{11}$  to be parallel to the  $C'_I-C'_I$  bond, while it may deviate from the bond direction by about  $10^\circ$  (Veeman et al., 1984). We found that this amount of deviation changes the best-fit values to  $(\phi_I, \psi_I) = (-76^\circ, 138^\circ)$ . The CSA parameters  $(\delta, \eta)$  were assumed to be  $(\delta, \eta) = (-68.9 \text{ ppm}, 0.93)$ , while they are  $(-72.8 \text{ ppm}, 0.94)$ ,  $(-71.0 \text{ ppm}, 0.84)$ ,  $(-68.7 \text{ ppm}, 0.84)$ ,  $(70.2 \text{ ppm}, 0.85)$ , and  $(-67.1 \text{ ppm}, 0.90)$  for glycine (Haberkmorn et al., 1981), L-alanine (Naito et al., 1981), L-serine (Naito et al., 1983), L-threonine (Janes et al., 1983), and L-asparagine (Naito et al., 1984), respectively. Using these CSA parameters, we obtained  $(\phi_I, \psi_I)$  to be  $(-76^\circ, 137^\circ)$ ,  $(-76^\circ, 143^\circ)$ ,  $(-75^\circ, 148^\circ)$ ,  $(-76^\circ, 149^\circ)$ , and  $(-76^\circ, 150^\circ)$ , for glycine, L-alanine, L-serine, L-threonine, and L-asparagine, respectively. These results show that the use of likely CSA tensors for  $C'_G$  and  $C'_I$  in the simulations causes little error in the determination of  $\phi_I$ , but leads to considerable error in  $\psi_I$ . Since the  $\phi_I$  value is directly related to the distance, it is insensitive to the CSA tensors, while the  $\psi_I$  value is related mainly to the relative orientations of the CSA tensor of the carbonyl carbon to the other tensor, being more sensitive to them. In fact, Tycko et al. showed that both  $\phi$  and  $\psi$  can be determined by correlating the two CSAs of the carbonyl carbons in adjacent amino acid residues (Tycko et al., 1996). To obtain a more precise value for  $\psi_I$ ,  $(\delta, \eta)$  for  $C'_I$  should be measured by some method.

In cyclic peptides or peptides with proline,  $\omega_G$  may be  $0^\circ$ , and therefore we examine the possibility of determining whether  $\omega_G = 0^\circ$  or  $180^\circ$ . Obtaining a similar rmsd contour plot for  $\omega_G = 0^\circ$ , we determined  $\phi_I$  and  $\psi_I$  to be  $-86^\circ$  and  $167^\circ$ , respectively. In Figure 5a is shown the recoupling-time dependence calculated for both best-fit parameter sets  $(\omega_G, \phi_I, \psi_I) = (180^\circ, -76^\circ, 147^\circ)$  and  $(0^\circ, -86^\circ, 167^\circ)$ . Unfortunately, the simulations for the two sets of dihedral



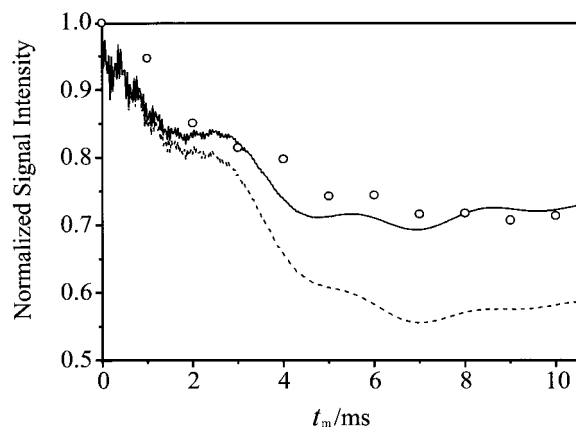


Figure 6. Recoupling-time dependence of the normalized magnetization of  $C_1'$  in 10% uniformly  $^{13}\text{C},^{15}\text{N}$ -labeled glycolisoleucine. The dipolar recoupling experiment was carried out using the pulse sequence in Figure 2a under an R2TR condition ( $\omega_{eI} + \omega_{eS} = \omega_R$ ) satisfied for  $C_1'$  and  $C_G^\alpha$  by applying an rf field with intensity 2800 Hz on-resonance to the  $C_1'$  carbon under MAS with  $\omega_R = 17.03$  kHz. Experimental points are shown by circles. The standard deviation for each point is ca.  $\pm 0.04$ . The solid line is the curve calculated for the dihedral angles  $(\omega_G, \phi_I, \psi_I) = (180^\circ, -76^\circ, 147^\circ)$ , whereas the dotted line for  $(\omega_G, \phi_I, \psi_I) = (0^\circ, -86^\circ, 167^\circ)$ .  $T_{1\rho}$  was determined to be 500 ms for  $C_1'$  in 10%  $^{13}\text{C},^{15}\text{N}$ -labeled glycolisoleucine, and used to correct the experimental data.

angles are similar, so that we cannot choose the correct set out of the two from this result. To conclude which set of dihedral angles is correct, we did another recoupling experiment for  $C_G^\alpha$  and  $C_1'$ . The recoupling-time dependence can be calculated for given  $\omega_G$ ,  $\phi_I$ , and  $\psi_I$ . An rf field with intensity 2800 Hz was applied on-resonance to the  $C_1'$  carbon which satisfies a DQ condition under spinning with  $\omega_R = 17.03$  kHz. Figure 6 shows the recoupling-time dependence of the magnetization of  $C_1'$  together with the simulated curves obtained for the above two sets of dihedral angles. Clearly, the former set reproduces the observation as expected. This indicates that even when we do not know whether  $\omega = 0^\circ$  or  $180^\circ$ , we can determine the three dihedral angles ( $\psi$ ,  $\omega$ ,  $\phi$ ) by two dipolar recoupling experiments per amino acid residue.

As shown here, the recoupling-time behavior in a general  $sp^2$ - $sp^2$   $^{13}\text{C}$  spin pair depends not only on the internuclear distance, but also on the relative orientations between the CSA tensors and the dipolar vector as well as the CSA parameters. Fortunately, the orientations and values for  $sp^2$  carbons have been well established and are virtually independent of peptides. Further, owing to the dependence caused by CSA, the magnitudes of not only  $\phi$  but also of  $\psi$  can be determined. Moreover,  $C_1^\alpha$  and  $C_1^\beta$  carbons also contribute

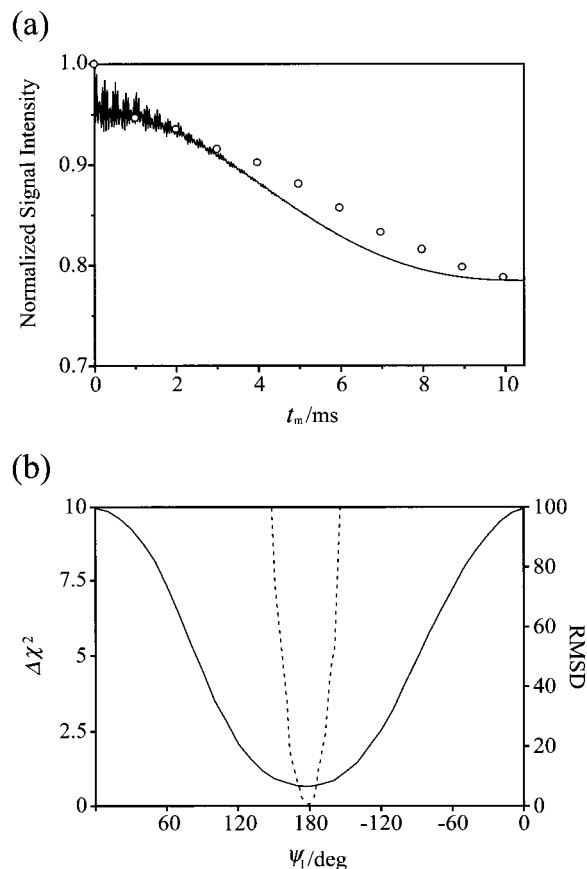


Figure 7. (a) Recoupling-time dependence of the normalized magnetization of  $C_1'$  in 10% uniformly  $^{13}\text{C},^{15}\text{N}$ -labeled glycolisoleucine. The dipolar recoupling experiment was carried out using the pulse sequence in Figure 2a under an R2TR condition ( $\omega_{eI} + \omega_{eS} = \omega_R$ ) satisfied for  $C_1'$  and  $C_1^{\gamma 1}$  by applying an rf field with intensity 2000 Hz on-resonance to the  $C_1'$  carbon under MAS with  $\omega_R = 17.46$  kHz. Experimental points are shown by circles. The standard deviation for each point is ca.  $\pm 0.03$ . The curves are calculated for the dihedral angle  $\chi_{II}$  of  $178^\circ$ .  $T_{1\rho}$  was determined to be 500 ms for  $C_1'$  in 10%  $^{13}\text{C},^{15}\text{N}$ -labeled glycolisoleucine, and used to correct the experimental data. (b) Dihedral angle ( $\chi_{II}$ ) dependence of rmsd (solid line) between the experimental (Figure 7a) and simulated data and of  $\Delta\chi^2$  (dashed line).

to the experimental result due to the incomplete selectivity; however, it provides the benefit of being able to determine the signs of  $\phi$  and  $\psi$ .

$\chi_{II}$  angle: The  $\chi_{II}$  angle was obtained by selective dipolar recoupling between  $C_1'$  and  $C_1^{\gamma 1}$ , which was attained by applying an rf field with intensity 2000 Hz on-resonance to the  $C_1'$  carbon under MAS with  $\omega_R = 17.46$  kHz. Figure 7a shows the observed recoupling-time dependence of the  $C_1'$  magnetization. Figure 7b indicates the rmsd between the experimental data and

the curves calculated for various  $\chi_{11}$ . We included  $C_1^\alpha$ ,  $C_1^\beta$ , and  $C_1^\delta$  besides  $C_1'$  and  $C_1^{\gamma 1}$  in the simulation, making the rmsd plot slightly asymmetric, as shown in Figure 7b. From the minimum,  $\chi_{11}$  was determined to be  $178^\circ$ . The recoupling-time dependence calculated for  $\chi_{11} = 178^\circ$  is shown in Figure 7a. The 68% confidence interval is  $\pm 10^\circ$ , as shown in Figure 7b, being large because  $\chi_{11} \sim 180^\circ$ .

Here, we examine the effect of the chemical shift tensors of  $C_1'$  and  $C_1^{\gamma 1}$ . We found that the above deviation of the  $\sigma_{11}$  direction for  $C_1'$  does not alter the best-fit value of  $178^\circ$ . Using the above parameters ( $\delta$ ,  $\eta$ ) for  $C_1'$  in glycine, L-alanine, L-serine, L-threonine, and L-asparagine, we obtained the best-fit values of  $\chi_{11}$  to be  $178^\circ$ ,  $178^\circ$ ,  $175^\circ$ ,  $178^\circ$ , and  $175^\circ$ , respectively. As for  $C_1^{\gamma 1}$ , it was found that changing the CSA orientation hardly affects the calculated recoupling-time dependence, while changing the CSA parameters ( $\delta$ ,  $\eta$ ) from  $(-12.3 \text{ ppm}, 0.58)$  for the  $\alpha$ -methylene carbon of *n*-eicosane (VanderHart et al., 1976), which was used for the simulation, to  $(-7.3 \text{ ppm}, 0.58)$  results in the best-fit value of  $\chi_{11} = -176^\circ$ .

As exemplified by the present case, in a general  $sp^3$ - $sp^2$   $^{13}\text{C}$  spin pair, possible variations of parameters and orientations of their CSA tensors barely affect the recoupling-time dependence. Thus, we may safely use likely CSA parameters ( $\delta$ ,  $\eta$ ) and tensor orientations for both carbons.

### 2D dipolar correlation experiment

$\chi_{12}$  angle: To determine the  $\chi_{12}$  angle in the same way, it is necessary to selectively recouple  $C_1^\alpha$  and  $C_1^\delta$ , or  $C_1^{\gamma 2}$  and  $C_1^\delta$ . However, since their chemical-shift values are very similar to each other and, moreover, the atomic positions are close to each other, selective recoupling of one of these pairs is difficult. In this sense, the isoleucine residue is one of the most demanding ones for the present approach. Therefore, we adopted another way of observing a  $C_1^\alpha$ - $C_1^\beta$ / $C_1^{\gamma 1}$ - $C_1^\delta$  dipolar correlation 2D powder pattern using the sequence shown in Figure 2b. The spinning speed  $\omega_R$  was set to 5110 Hz, satisfying the  $R^2$  condition for  $C_1^\delta$  and  $C_1^\alpha$ . In the  $t_1$  period, a DQ condition is matched for  $C_1^{\gamma 1}$  and  $C_1^\delta$  by applying an rf field with intensity 2540 Hz on-resonance to  $C_1^\delta$ . During the mixing time  $t_m$ , the magnetization of  $C_1^\delta$  is selectively transferred to  $C_1^\alpha$  by  $R^2$ . In the  $t_2$  period, a DQ condition is fulfilled for  $C_1^\alpha$  and  $C_1^\beta$  by applying an rf field with intensity 1825 Hz on-resonance to  $C_1^\alpha$ .

Figure 8a shows the experimental spectrum, which was observed using a 100% uniformly labeled sample for obtaining a high signal-to-noise ratio. The use of the undiluted sample is justified, because in this experiment, the dipolar interactions recoupled in the  $t_1$  and  $t_2$  periods are of directly bonded nuclei, and thus much stronger than the intermolecular dipolar interactions. We simulated 2D spectra for various  $\chi_{12}$  angles, including  $C_1^{\gamma 2}$  in addition to  $C_1^\alpha$ ,  $C_1^\beta$ ,  $C_1^{\gamma 1}$  and  $C_1^\delta$ . In the course of our study, we found that the  $C_1^{\gamma 1}$ - $C_1^\delta$  bond apparently shows an unusual bond length, which may be caused by a large vibration of  $C_1^\delta$ . With the existence of molecular motion, dihedral angles cannot be correctly determined from distance measurements. However, in a theoretical study of vibrational effects (Ishii et al., 1997), it has been proven that the dipolar 2D powder patterns provide correct dihedral angles even under the presence of molecular vibrations as long as the asymmetry of the vibration is negligible. It is a common problem for various methods of structure determination that we must pay attention to the presence of local motion. Figure 8b shows the  $\chi_{12}$  dependence of rmsd between the experimental and calculated 2D spectra. From the minimum,  $\chi_{12}$  was determined to be  $160^\circ$ , and the spectrum calculated with  $\chi_{12} = 160^\circ$  is given in Figure 8a. In this simulation, a somewhat long bond length of 1.62 Å was assumed for the  $C_1^{\gamma 1}$ - $C_1^\delta$  bond, corresponding to our observation of the unusual vibration of  $C_1^\delta$ , which provides the best agreement with the experimental spectrum. Even though the agreement is not excellent, the  $\Delta\chi^2$  plot (Ishii et al., 1998) in Figure 8b shows that the 68% confidence interval is  $\pm 5^\circ$ . The sign of  $\chi_{12}$  cannot be determined from this experiment. We calculated the dihedral angle ( $C_1^{\gamma 2}$ - $C_1^\beta$ - $C_1^{\gamma 1}$ - $C_1^\delta$ ) to be  $39^\circ$  from  $\chi_{12} = -160^\circ$ , and to be  $79^\circ$  from  $\chi_{12} = 160^\circ$ ; this suggests that the steric hindrance between the two methyl groups is smaller for the latter case. Therefore, we prefer the positive sign.

In these simulations, chemical shift anisotropies are not included; we found that even if likely chemical shift tensors are included; the spectrum does not change appreciably, under the MAS frequency of  $\sim 5$  kHz. This is fortunate, because the CSA tensors of  $sp^3$  carbons depend heavily on circumstances, so that it is very difficult to assume them appropriately for simulations.

For a directly bonded  $sp^3$ - $sp^3$   $^{13}\text{C}$  spin pair, the effect of CSAs can indeed be neglected in comparison with the contribution of the dipolar coupling under MAS with a spinning speed a few times faster than  $|\delta|$ ,

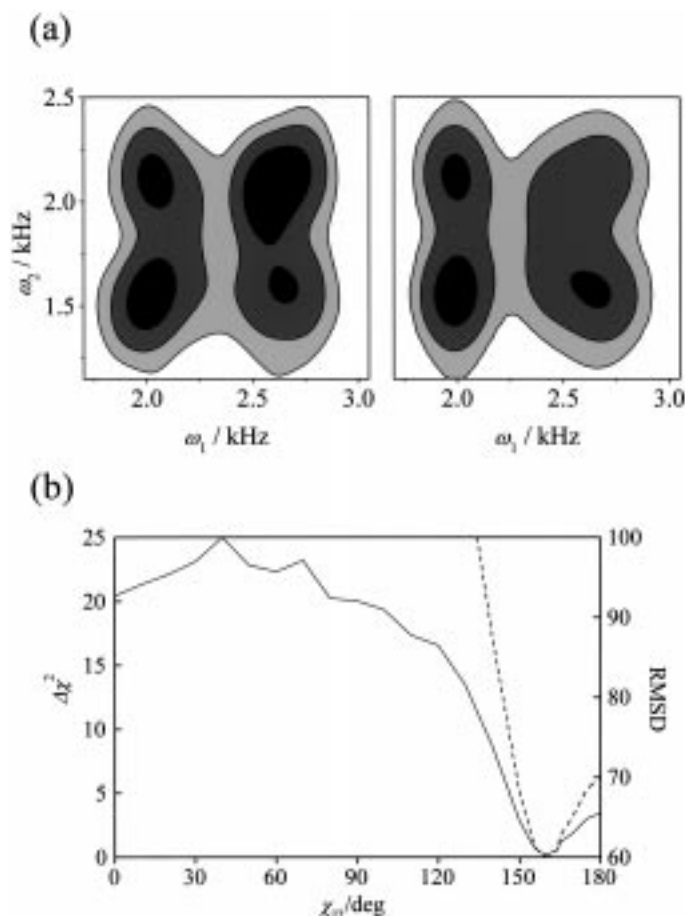


Figure 8. (a) The 2D  $C_1^\alpha-C_1^\delta/C_1^{\gamma 2}-C_1^\delta$  dipolar correlation spectrum for uniformly  $^{13}\text{C},^{15}\text{N}$ -labeled glycyloisoleucine. The experiment was performed using the pulse sequence in Figure 2b. The spinning frequency  $\omega_R$  is 5110 Hz. The  $^{13}\text{C}$  rf-field intensities during the  $t_1$  period, the mixing time, and the  $t_2$  period are  $\omega_1/2 = 2540$  Hz (on-resonance to the  $C_1^\delta$  carbon), 0 Hz, and 1825 Hz (on-resonance to the  $C_1^\alpha$  carbon), respectively. Left: experimental 2D spectrum; right: simulated 2D spectrum calculated for the  $C_1^{\gamma 1}-C_1^\delta$  distance of 1.62 Å and the dihedral angle  $\chi_{12}$  of  $160^\circ$ . The contour lines are plotted at 65%, 77%, and 88% of the maximum intensity. (b) Dihedral angle ( $\chi_{12}$ ) dependence of rmsd (solid line) between the experimental (Figure 8a) and simulated 2D dipolar correlation spectra and of  $\Delta\chi^2$  (dashed line).

according to our simulations. On the other hand, for a nonbonded, namely weakly dipolar coupled  $\text{sp}^3\text{-sp}^3$   $^{13}\text{C}$  spin pair, the effect of the CSAs becomes more important than for a directly bonded pair. Therefore, the CSA effect must be reduced for accurate determination of dihedral angles by using a sufficiently fast spinning speed. Then a large  $\omega_1$  is needed to satisfy a DQ recoupling condition, so that selectivity is declined. Therefore, when some other  $\text{sp}^3$  carbons exist close to the relevant carbons, the dipolar recoupling experiment (Figure 2a) does not work well, and the 2D dipolar correlation experiment (Figure 2b) is recommended.

### Three-dimensional structure

Figure 9a shows the 3D structure constructed from the dihedral angles determined by the present R2TR experiments. For comparison, we have also made an X-ray structural analysis; no X-ray structure of glycyloisoleucine has been reported. Figure 9b shows the structure by X-ray crystallography. The dihedral angles determined by NMR and X-ray are  $(\psi_G, \omega_G, \phi_I, \psi_I, \chi_{II}, \chi_{12}) = (180^\circ, 180^\circ, -76^\circ, 147^\circ, 178^\circ, 160^\circ)$  and  $(165^\circ, 170^\circ, -70^\circ, 156^\circ, 178^\circ, 170^\circ)$ , respectively. Although of course the result by NMR includes errors, the X-ray structure is not very accurate either: we could not prepare a good sample for the X-ray structural analysis. Nevertheless, both structures are in good agreement, indicating that the present ap-

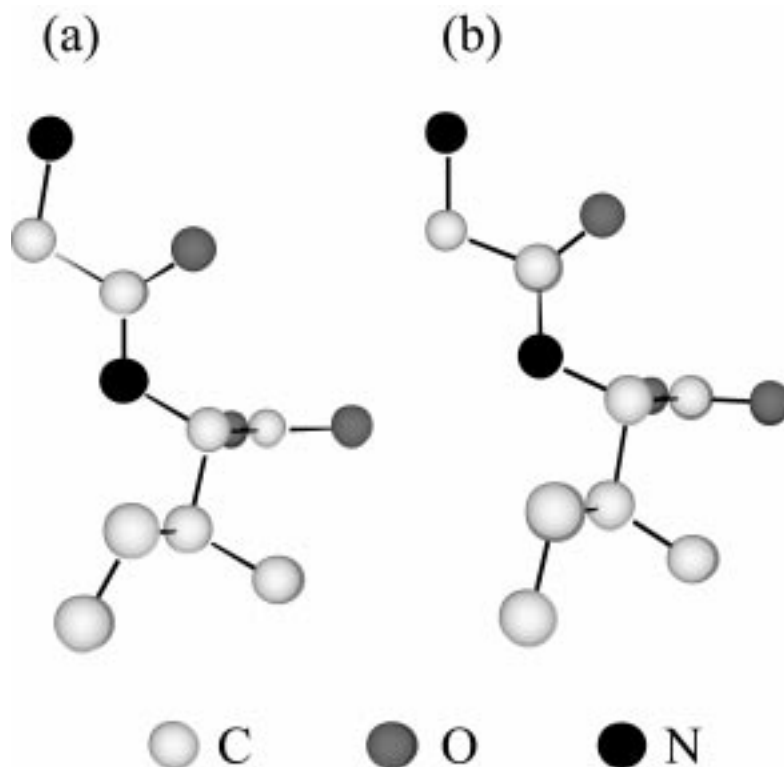


Figure 9. Three-dimensional structure of glycylisoleucine. (a) Present NMR study. (b) X-ray crystallography.

proach is useful for structure determination. Further, the X-ray diffraction showed that the thermal vibration parameters of  $C_1^\delta$  are very large, agreeing with our observation by NMR.

### Conclusions

In this work, we have determined the complete 3D structure of a uniformly  $^{13}C,^{15}N$ -labeled Gly-Ile molecule using the R2TR method, by which all the dihedral angles were individually determined by selectively recoupling some dipolar interactions between three- or four-bonds distant spins or observing a dipolar correlation 2D powder pattern. Choosing three adjustable parameters  $\omega_1$ ,  $\omega_0$ , and  $\omega_R$  properly, we could find a R2TR condition suitable for selective recoupling of the pair of spins concerned. Furthermore, it is not always necessary that all resonances are resolved; it is possible to monitor the recoupling-time dependence if only one of the pair of spins concerned is resolved well from the others.

The present approach can be applied to determine the 3D structure of a small molecule and also the struc-

ture of a restricted region important to the biological function of a large system using a sample in which the region is uniformly or multiply labeled. So far quantitative structural information obtained by solid state NMR has been almost limited to a single inter-nuclear distance or dihedral angle. The present approach increases the obtainable quantity of structural information in a single powder sample.

### Acknowledgements

K.N. thanks the Japan Society Promotion of Science for the research fellowship. This research was supported by a Grant-in-Aid for Science Research.

### References

- Andrew, E.R., Bradbury, A., Eades, R.G. and Wynn, V.T. (1963) *Phys. Lett.*, **4**, 99–100.
- Andrew, E.R., Clough, S., Farnell, L.F., Gledhill, T.D. and Roberts, I. (1966) *Phys. Lett.*, **21**, 505–506.
- Bennett, A.E., Ok, J.H., Griffin, R.G. and Vega, S. (1992) *Chem. Phys. Lett.*, **96**, 8624–8627.

- Bennett, A.E., Rienstra, C.M., Auger, M., Lakshmi, K.V. and Griffin, R.G. (1995) *J. Chem. Phys.*, **103**, 6951–6958.
- Brenner, M. and Winitz, W. (1953) *Helv. Chim. Acta*, **36**, 1109–1115.
- Facelli, J.C., Orendt, A.M., Solum, M.S., Depke, G., Grant, D.M. and Michl, J. (1986) *J. Am. Chem. Soc.*, **108**, 4268–4272.
- Fujiwara, T., Ramamoorthy, A., Nagayama, K., Hioka, K. and Fujito, T. (1993) *Chem. Phys. Lett.*, **212**, 81–84.
- Gullion, T. and Schaefer, J. (1989) *J. Magn. Reson.*, **81**, 196–200.
- Gullion, T. and Vega, S. (1992) *Chem. Phys. Lett.*, **194**, 423–428.
- Haberkorn, R.A., Stark, R.E., van Willigen, H. and Griffin, R.G. (1981) *J. Am. Chem. Soc.*, **103**, 2534–2539.
- Ishii, Y. and Terao, T. (1995) *J. Magn. Reson.*, **A115**, 116–118.
- Ishii, Y., Terao, T. and Hayashi, S. (1997) *J. Chem. Phys.*, **107**, 2760–2774.
- Ishii, Y., Hirao, K., Terao, T., Terauchi, T., Oba, K., Nishiyama, M. and Kainosho, M. (1998) *Solid State NMR*, **11**, 169–175.
- Janes, N., Ganapathy, S. and Oldfield, E. (1983) *J. Magn. Reson.*, **54**, 111–121.
- Könich, W. and Geiger, R. (1970) *Chem. Ber.*, **103**, 788–798.
- Levitt, M.H., Raleigh, D.P., Creuzet, F. and Griffin, R.G. (1990) *J. Phys. Chem.*, **92**, 6347–6364.
- Lee, Y.K., Kurur, N.D., Helmle, M., Johannessen, O.G., Nielsen, N.C. and Levitt, M.H. (1995) *Chem. Phys. Lett.*, **223**, 304–309.
- Moroder, L., Hallett, A., Wünsch, E., Keller, O. and Wersin, G. (1976) *Hoppe-Seyler's Z. Physiol. Chem.*, **357**, 1651–1653.
- Naito, A., Ganapathy, S., Akasaka, K. and McDowell, C.A. (1981) *J. Chem. Phys.*, **74**, 3190–3197.
- Naito, A., Ganapathy, S., Raghunathan, P. and McDowell, C.A. (1983) *J. Chem. Phys.*, **79**, 4173–4182.
- Naito, A. and McDowell, C.A. (1984) *J. Chem. Phys.*, **81**, 4795–4803.
- Nishimura, K., Naito, A., Tuzi, S., Saito, H., Hashimoto, C. and Aida, M. (1998) *J. Phys. Chem.*, **102**, 7476–7483.
- Nomura, K., Takegoshi, K., Terao, T., Uchida, K. and Kainosho, M. (1999) *J. Am. Chem. Soc.*, **121**, 4064–4065.
- Oas, T.G., Hartzell, C.J., McMahon, T.J., Drobny, G.P. and Dahlquist, F.W. (1987a) *J. Am. Chem. Soc.*, **109**, 5956–5962.
- Oas, T.G., Hartzell, C.J., Dahlquist, F.W. and Drobny, G.P. (1987b) *J. Am. Chem. Soc.*, **109**, 5962–5966.
- Raleigh, D.P., Harbison, G.S., Neiss, T.G., Roberts, J.E. and Griffin, R.G. (1987) *Chem. Phys. Lett.*, **138**, 285–290.
- Raleigh, D.P., Levitt, M.H. and Griffin, R.G. (1988) *Chem. Phys. Lett.*, **146**, 71–76.
- Roberts, J.E., Harbison, G.S., Munowitz, M.G., Herzfield, J. and Griffin, R.G. (1987) *J. Am. Chem. Soc.*, **109**, 4163–4169.
- Sun, B.Q., Costa, P.R., Kocisko, D., Lansbury, P.T.J. and Griffin, R.G. (1995) *J. Chem. Phys.*, **102**, 702–707.
- Takegoshi, K., Nomura, K. and Terao, T. (1995) *Chem. Phys. Lett.*, **232**, 424–428.
- Takegoshi, K., Takeda, K. and Terao, T. (1996) *Chem. Phys. Lett.*, **260**, 331–335.
- Takegoshi, K., Nomura, K. and Terao, T. (1997) *J. Magn. Reson.*, **127**, 206–216.
- Tycko, R. and Dabbagh, G. (1990) *Chem. Phys. Lett.*, **173**, 461–465.
- Tycko, R., Weliky, D.P. and Berger, A.E. (1996) *J. Chem. Phys.*, **105**, 7915–7930.
- VanderHart, D.L. (1976) *J. Chem. Phys.*, **64**, 830–834.
- Veeman, W.S. (1984) *Prog. NMR Spectrosc.*, **16**, 193–235.